
Improving the Reasoning of Multi-Image Grounding in MLLMs via Reinforcement Learning

Bob Zhang^{1*} , **Haoran Li**^{1,2*} , **Tao Zhang**³ , **Cilin Yan**¹ , **Jiayin Cai**¹ **Xiaolong Jiang**¹ , **Yanbin Hao**^{4†}

¹Xiaohongshu Inc.

²University of Science and Technology of China

³Wuhan University

⁴Hefei University of Technology

Abstract

Recently, Multimodal Large Language Models (MLLMs) excel at visual grounding in single-image scenarios with textual references. However, their performance degrades when handling real-world applications involving complex multi-image compositions and multimodal instructions, which reveals limitations in cross-image reasoning and generalization. To address these challenges, we adopt a Reinforcement Learning (RL) based post-training strategy to improve the reasoning performance of MLLMs in multi-image grounding tasks. Our approach begins with synthesizing high-quality chain-of-thought (CoT) data for cold-start initialization, followed by supervised fine-tuning (SFT) using low-rank adaptation (LoRA). The cold-start training stage enables the model to identify correct solutions. Subsequently, we perform rejection sampling using the merged SFT model to curate high-quality RL data and leverage rule-based RL to guide the model toward optimal reasoning paths. Extensive experimental results demonstrate the effectiveness of our approach, achieving +9.04% improvements on MIG-Bench and +4.98% improvements on several out-of-domain reasoning grounding benchmarks over the SFT baseline. Furthermore, our approach exhibits strong generalization in multi-image perception, with gains of +3.1% and +2.4% over the base model on subsets of the BLINK and MMIU benchmarks, respectively.

1 Introduction

The traditional visual grounding task focuses on localizing target regions within a single image using simple natural language descriptions. Recent research leveraging large language models (LLMs) has significantly improved performance on this task by utilizing LLMs' powerful language comprehension capabilities. However, real-world applications often require sophisticated multi-image grounding with complex instructions, including cross-image reasoning. As illustrated in Figure 1, practical scenarios often require identifying the region that best matches the semantics of the query image. Such tasks demand advanced multi-modal reasoning and comprehensive understanding across multiple visual contexts.

Recently, Migician [19] introduces a multi-image grounding dataset with the MIG-Bench benchmark. By employing a two-stage supervised fine-tuning (SFT) pipeline on their dataset, they have achieved impressive results, demonstrating the potential of MLLMs for multi-image grounding tasks. However, their SFT-based approach primarily “memorize” [4] understanding patterns and instruction-following behaviors in multi-image scenarios, rather than developing robust reasoning capabilities. This limitation constrains the model’s ability to generalize to novel scenarios and real-world applications.

*Equal contributions, †Corresponding author.

Question

Ground the object in Image-2 that is mostly required by the person in Image-1. Find it and locate it in the second image.

Ours Reasoning-based Answer

<think> To solve this, we need to identify the object in Image-2 that is most relevant to the person in Image-1, who appears to be cold and possibly in a cold environment.

1. **Identify the person's needs:** The person in Image-1 is wearing a heavy coat and hat, suggesting they are cold. They might need something to keep warm or protect them from the cold.

2. **Analyze Image-2:** Image-2 shows a workshop setting with various tools and materials, including gloves, a tape measure, and wood. These items are related to construction or DIY work.

3. **Match needs with Image-2:** *Among the items in Image-2, the gloves are the most relevant. They are used for protection and warmth, which aligns with the person's need in Image-1.*

4. **Locate the gloves in Image-2:** The gloves are clearly visible in the foreground of Image-2, resting on a surface.

Based on this reasoning, the gloves in Image-2 are the most relevant object for the person in Image-1. *</think>*

<answer> json\n[{"bbox_2d": [22, 264, 322, 513], "label": "gloves"}] *</answer>*

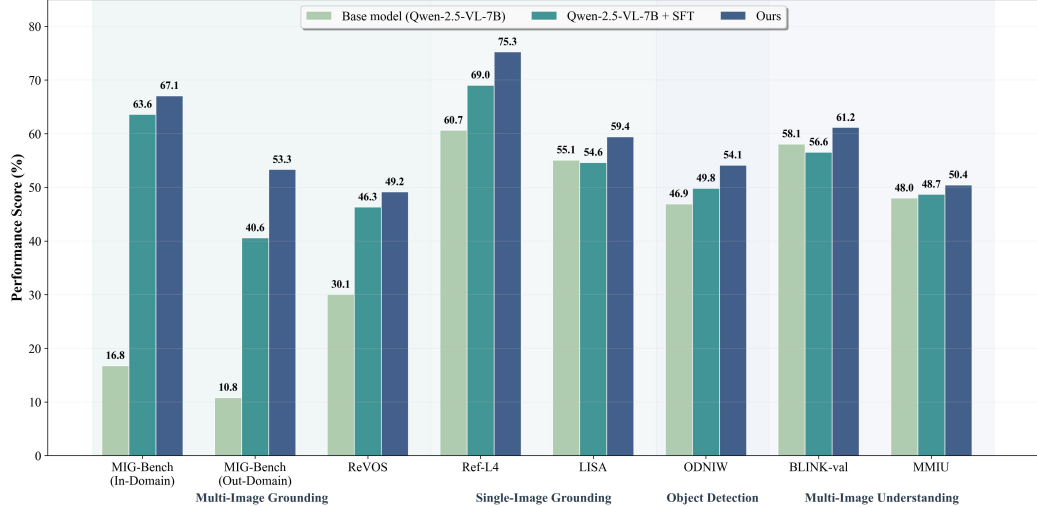


Figure 1: **Top:** Examples of our multi-image reasoning grounding. **Bottom:** The comparison of Qwen2.5-VL-7B model, SFT model, and our reasoning model. Our method achieves the best performance among all benchmarks.

Inspired by the recent success in RL-based post-training frameworks for Large Reasoning Models (LRM) [10, 35, 41], we explore the potential of the RL paradigm to improve the reasoning abilities of MLLMs in multi-image grounding scenarios. Our preliminary attempts applied RL directly to the state-of-the-art open-source MLLM, Qwen2.5-VL-7B [1]. However, we found that the model often failed to generate correct responses during the RL training stage, which we attribute to two key limitations of the base model: (1) inadequate capacity for processing complex image queries, and (2) insufficient ability to handle multi-image contexts. It suggests that directly employing RL paradigm on the base model is ineffective for exploring reasoning paths in such challenging scenarios.

To overcome these limitations, we synthesize high-quality chain-of-thought (CoT) data for cold-start initialization using large-scale MLLMs, Qwen2.5-VL-7B. This data serves for supervised fine-tuning (SFT) with low-rank adaptation (LoRA), enabling the model to develop robust multi-image comprehension and reasoning capabilities. Then, we remove low-quality data through rejection sampling according to predictions from the merged cold-start SFT model. Finally, we employ a rule-based RL paradigm based on Group Relative Policy Optimization (GRPO) [32] to guide the model toward discovering correct reasoning paths while improving generalization performance.

We conduct comprehensive experiments on several benchmarks to demonstrate the effectiveness of our training pipeline. On the multi-image grounding benchmark MIG-Bench [19], our model achieves improvements of +3.46% (in-domain) and +12.76% (out-of-domain) over the SFT baseline. For zero-shot grounding evaluation, our approach outperforms the SFT baseline by +6.23% on Ref-L4 [2], +4.79% on LISA-Grounding [15], and +2.83% on ReVOS-Grounding [40]. Furthermore, for the multi-image understanding benchmarks, our approach exhibits strong generalization capabilities, with improvements of +3.1% on BLINK [9] and +2.4% on MMIU [26] compared to the base Qwen2.5-VL-7B model.

2 Related Works

2.1 MLLM-based Referring Grounding.

Referring grounding, also known as referring expression comprehension (REC), involves identifying a specific object within an image based on a given referring natural language expression. With the rapid advancement of multimodal large language models (MLLMs) [22, 37, 16, 13, 17, 1, 51], significant progress has been made in extending their capabilities to address more challenging tasks, including fine-grained image understanding, object detection [47, 14], and visual grounding [15, 40, 31, 20]. Although these MLLMs have achieved strong performance on standard benchmarks such as RefCOCO/+g [25, 46], their visual grounding capabilities remain largely confined to single-image contexts and face substantial difficulties in capturing cross-image relationships. Recent efforts, such as Migician [19], introduce multi-image grounding tasks and further propose a two-stage supervised fine-tuning strategy, achieving notable results in these tasks. However, such approaches still exhibit insufficient reasoning abilities and limited generalization in multi-image and out-of-domain settings. In this paper, we explore the potential of the RL paradigm to improve the reasoning and comprehension abilities of MLLMs in multi-image grounding scenarios.

2.2 Reinforcement Learning-based Reasoning Model

Recent advancements in improving the reasoning ability of large language models [12, 39, 7, 10, 35] have been made through Chain-of-Thought (CoT) training or reinforcement learning-based post-training. Previous methods, such as Reinforcement Learning from Human Feedback (RLHF) [28] and Direct Preference Optimization (DPO) [30], have explored aligning models with human preferences, achieving remarkable success in enhancing reasoning and instruction-following capabilities. Recently, DeepSeek-R1 [10] employed the Group Relative Policy Optimization (GRPO) [32] algorithm as a post-training method without the need for critic models, demonstrating the potential of large-scale reinforcement learning. Inspired by the success of DeepSeek-R1, a series of subsequent works rapidly adopted this approach to enhance multi-modal reasoning across various domains, including mathematical problem solving [42, 29, 11, 49, 6], video understanding [8, 50, 21, 38], and visual perception tasks [33, 23, 5, 24, 48, 45, 34]. Among the most closely related works to ours, VLM-R1 [33], Visual-RFT [24], Vision-R1 [48], Perception-R1 [45], most focus exclusively on single-image visual grounding or object detection. However, these approaches lack the capability for multi-image perception and reasoning. In this paper, we follow the DeepSeek-R1 paradigm and extend it to the multi-image grounding tasks, while also achieving strong performance on single-image grounding and multi-image understanding tasks.

3 Method

3.1 Basic Settings

We begin by formally defining the multi-image grounding task. Formally, given a natural language description t , a query image Q , and several target images $\{I_1, I_2, \dots, I_m\}$, the model M is required to generate a bounding box G that indicates the region satisfying the semantic and contextual constraints specified by t and Q .

Unlike conventional grounding tasks that rely on fixed instruction templates, multi-image grounding involves dynamic and flexible instructions, which demand significantly stronger instruction comprehension and reasoning capabilities from MLLMs. To address the challenge, we introduce a

reinforcement learning training strategy to enhance the model’s reasoning capabilities, inspired by recent breakthrough improvements in LRM. We employ Qwen2.5-VL-7B as the base model due to its excellent multi-modal comprehension performance. Our RL paradigm is similar to DeepSeek-R1 [10], consisting of cold-start CoT-SFT initialization, rejection sampling, and rule-based RL training. We will provide detailed descriptions of our dataset construction strategy and training paradigm in the following subsections.

3.2 Cold Start Initialization

As analyzed in DeepSeek-R1 [10], directly applying reinforcement learning (RL) from scratch may cause the model to enter an unstable state. Specifically, the base MLLM model struggles to handle complex multi-image contexts and accurately localize target regions within multi-image scenarios. To mitigate these issues, it is crucial to pre-equip the model with task-specific reasoning capabilities before RL fine-tuning. We achieve this by constructing a high-quality CoT cold-start dataset, which provides structured reasoning guidance to bootstrap the model’s initial performance.

Task	Subsets	Number	Source
Mulit-image Grounding	Common Object	22k	
	Referring Grounding	24k	MGrounding-630k
	Region Locating	5k	
	Static Difference	3k	
Single-image Grounding	-	1k	Refcoco/g/+
		1k	ODINW, V3DET

Table 1: Details of constructed CoT cold-start dataset.

3.2.1 Chain-of-Thought Reasoning Data Collection

We construct our CoT dataset primarily based on MGrounding-630k dataset [19]. To maintain the model’s capability in single-image grounding scenarios, additionally introduce a small amount of single-image grounding data, including RefCOCO/+g [25, 46], as well as data from other sources, such as ODINW [18] and V3Det [36].

We utilize the advanced large-scale MLLM Qwen2.5-VL-72B to generate CoT reasoning data. Given a question, along with images and a fixed prompt similar to DeepSeek-R1, the model generates CoT rationales processes in the following format:

- {Question} First output the thinking process in `<think> </think>` tags and then output the final answer in `<answer> </answer>` tags. Output the bounding box coordinates in JSON format.

To improve data quality, we conduct an additional data filtering strategy. For each sample, we prompt the model to produce four distinct responses. Then, We estimate the difficulty of each sample based on the Intersection over Union (IoU) accuracy among these four responses, retaining only samples for which the accuracy is 1 to ensure the reliability of the data. After filtering, we obtain 56k high-reliability CoT cold-start samples, with detailed statistics presented in Table 1.

3.2.2 Supervised Fine-tuning

Leveraging our CoT cold-start dataset, we perform fine-tuning of the Qwen2.5-VL model to develop its multi-image comprehension and reasoning capabilities. During this training phase, we implement strong supervision via next-token prediction across the entire generation process, effectively incorporating knowledge at both the reasoning trace level and the final bounding box prediction.

We recognize that conventional full-parameter fine-tuning risks locking the model into rigid reasoning patterns, which could compromise both its generalization capacity and conversational fluency. To address this, we employ the LoRA fine-tuning approach, which maintains the model’s foundational knowledge while significantly enhancing its perception and reasoning performance in multi-image

grounding tasks. Then we merge the LoRA parameters with the original base model, yielding our stage-1 CoT-SFT model.

3.3 Reinforcement Learning

In the second stage, we implement GRPO [32], a rule-based reinforcement learning training paradigm, to further enhance the model’s reasoning capabilities. The model samples multiple candidate responses for each sample and are encouraged to reinforce responses achieving higher task-level rewards during GRPO training stage. To be specific, our model generates a group of G complete responses $\{o_1, o_2, \dots, o_G\}$ with current parameter group π_θ . Each response contains a full CoT reasoning process and a final bounding box prediction. For each o_i , we compute a scalar reward r_i , and normalize these rewards to estimate group-relative advantages A_i , formally as:

$$A_i = \frac{r_i - \text{mean}(\{r_j\}_{j=1}^N)}{\text{std}(\{r_j\}_{j=1}^N)} \quad (1)$$

Then, the training objective is given as follows:

$$\mathcal{J}_{GRPO}(\theta) = \frac{1}{N} \sum_{i=1}^N \left(\frac{\pi_\theta(o_i|q)}{\pi_{\theta_{old}}(o_i|q)} A_i - \beta \mathcal{KL}(\pi_\theta(o_i|q) \mid \pi_{ref}(o_i|q)) \right) \quad (2)$$

where $\pi_{\theta_{old}}$ and π_{ref} are the parameter groups of old model without latest updating and the fixed stage-1 CoT-SFT model. The parameter ϵ is used to control the clipping range, and β is the KL penalty coefficient.

Rejection Sampling To ensure efficient training, we implement a rejection sampling strategy based on our stage-1 CoT-SFT model. Specifically, we perform multiple sampling on the RL training data and remove samples where the model’s predictions are all correct or wrong. This approach is adopted because samples that the model answers either completely incorrectly or completely correctly do not contribute effectively to the relative advantage estimation in the GRPO algorithm. Retaining only samples where the model provides partially correct answers enables more efficient model optimization. After rejection sampling, we collect 174k data for stage-2 training.

To optimize the training efficiency of our reinforcement learning framework, we employ a rejection sampling strategy using our stage-1 CoT-SFT model. Specifically, we generate multiple predictions for each sample in the RL training dataset. Those samples where all predictions are correct or wrong are removed, as they contribute poorly to the relative advantage estimation in GRPO. On the other hand, partially correct samples offer optimal learning signals for model improvement. After applying this rigorous filtering process, we obtain a high-quality dataset of 174,000 samples for stage-2 RL training.

Reward Function We employ two reward functions for the multi-image grounding task: accuracy reward r_{acc} and format reward r_{format} .

Accuracy Reward. Given the ground truth bounding box B and the predicted bounding box \hat{B} , we calculate the $IoU(B, \hat{B})$ as our accuracy reward, where IoU denotes the Intersection over Union metric.

Format Reward. We adopt a format reward similar to that used in DeepSeek-R1, where the model output must follow the format: “<think>...</think><answer>...</answer>”. The reward score is set to 1 only when the output adheres to the required format; otherwise, the score is 0. Additionally, we impose constraints on the bounding box to ensure it is output in the correct JSON format.

The total reward is computed as a weighted sum of the accuracy and format rewards:

$$r = \lambda_{acc} r_{acc} + \lambda_{format} r_{format} \quad (3)$$

where λ_{acc} and λ_{format} denote the weights assigned to the accuracy reward and the format reward, respectively.

Models	Spontaneous Grounding			Referential Grounding						AVG	
	Difference		Similarity	Visual Reference			Textual	Visual+Textual			
	Static	Robust	Common	OT	MV	Region Refer	GG	Reason	Co-Re		
Human Performance											
Human	99.50*	97.87	98.00*	100.00	96.88	100.00*	98.99	91.06*	92.08	97.44	97.18
70B-Scale MLLMs											
LLaVA-OV-72B	13.26	5.34	26.84	12.91	7.64	2.14	17.83	21.60	11.88	8.55	13.65
InternVL2-76B	15.91	10.64	36.40	30.73	20.83	5.74	46.46	41.28	32.67	26.50	26.72
InternVL3-78B	10.04	9.57	24.12	27.08	14.58	10.44	50.51	38.08	45.54	17.09	24.71
Qwen2-VL-72B	46.12	46.81	64.46	26.73	22.57	18.62	33.33	62.53	50.50	17.09	38.88
Qwen2.5-VL-72B	43.75	46.81	69.98	34.32	29.17	8.31	62.63	59.92	66.34	41.03	46.23
7B-Scale MLLMs											
Mantis	1.52	0.00	3.31	12.18	2.08	1.00	1.01	10.02	0.00	0.85	3.20
LLaVA-OV-7B	6.06	3.19	3.43	0.18	1.04	1.08	9.09	15.43	6.93	0.85	4.73
Minicpm2.6	14.58	2.13	14.34	9.82	6.25	1.75	11.11	10.02	2.97	2.56	7.55
mPLUG-Owl3	18.56	6.38	34.93	8.55	7.64	2.41	7.07	22.85	9.09	5.98	12.35
InternVL2-8B	6.92	7.45	25.49	20.73	9.72	3.49	28.28	30.26	17.82	9.40	15.96
InternVL3-8B	23.67	14.89	47.99	14.84	6.94	12.13	7.07	34.87	16.83	2.56	18.18
Qwen2-VL-7B	27.84	38.30	19.36	20.73	11.81	25.95	23.23	58.52	48.51	11.97	28.62
Qwen2.5-VL-7B	28.03	5.32	21.81	15.23	5.56	4.07	13.13	32.26	3.96	2.56	13.19
+ SFT	53.22	44.68	82.11	26.59	35.07	39.32	79.80	59.72	53.47	23.93	49.79
+ CoT-SFT	47.35	<u>45.74</u>	76.59	46.14	34.03	28.93	80.81	63.93	66.34	34.19	52.41
Ours-GRPO	<u>51.52</u>	43.62	82.48	63.41	<u>38.54</u>	51.45	82.83	69.54	67.33	37.61	<u>58.83</u>

Table 2: **Performance comparison of different models on MIG-Bench.** OT, MV, GG, and Co-Re respectively mean object tracking, multi-view grounding, group grounding, and correspondence. For values marked with *, we randomly sample 20% testing examples for human evaluation on the corresponding task. The best and second-best results are marked in **bold** and underline, respectively.

Models	In-Domain	Out-of-Domain	AVG
Qwen2.5-VL-72B	46.17	46.27	46.23
Qwen2.5-VL-7B	16.76	10.82	13.19
+ SFT	63.61	40.58	49.79
+ CoT-SFT	58.42	48.40	52.41
Ours	67.07	53.34	58.83

Table 3: **In-domain vs Out-of-domain performance comparison on MIG-Bench [19].** The in-domain subsets include static difference, common object recognition, region localization, and referential grounding, while the out-of-domain subsets comprise robust difference, object tracking, multi-view grounding, group grounding, and correspondence.

4 Experiments

In this section, we first describe the implementation details of our approach in Section 4.1: benchmarks, baselines, and evaluation metrics. Subsequently, we present the comparison results in Section 4.2.

4.1 Implementation Details

Benchmarks We evaluate our method on the multi-image grounding benchmark MIG-Bench [19], object detection dataset ODINW [18], single-image grounding datasets: Ref-L4 [2], LISA-Grounding [15], and the video grounding dataset ReViOS Grounding [40]. ODINW comprises 13 distinct real-world settings featuring rare object categories, assessing the model’s object perception and inference ability in practical scenarios. Moreover, to further evaluate out-of-domain generaliza-

Model	Single image Grounding				Multi-image Grounding		AVG
	Ref-L4(val)	Ref-L4(test)	LISA(val)	LISA(test)	ReVOS		
Qwen2.5-VL-72B	74.85	76.71	53.57	46.85	48.78		60.15
Qwen2.5-VL-7B + SFT	58.57 68.92	62.76 69.14	<u>56.63</u> 55.10	53.54 <u>54.18</u>	30.07 46.33		52.31 58.73
Ours	74.78	75.74	62.76	56.11	49.16		63.71

Table 4: **Zero-shot evaluation on several reasoning grounding benchmarks:** Ref-L4 [2], LISA-Grounding [15], and ReVOS [40]. The best and second-best results are marked in **bold** and underline, respectively.

Method	OxfordPets	PascalVOC	WildfireSmoke	OpenPoetryVision	Vector	AVG
Qwen2.5-VL-72B	19.36	90.56	38.78	16.85	61.11	45.33
Qwen2.5-VL-7B + SFT	18.52 19.22	90.56 91.26	26.53 34.69	15.59 15.05	83.33 88.89	46.91 49.82
Ours	20.61	91.73	45.58	18.37	94.44	54.15

Table 5: **Out-of-domain object detection evaluation on ODNIW [18] dataset.** We individually employ five non-overlapping subsets: Oxford Pets, Pascal VOC, Wildfire Smoke, Open Poetry Vision, and Vector. The best result is indicated in **bold**.

tion ability of our model, we individually employ five non-overlapping subsets from ODINW: Oxford Pets, Pascal VOC, Wildfire Smoke, Open Poetry Vision, and Vector. Ref-L4 is a large-scale referring expression benchmark with diverse object categories, instance scales, and long textual descriptions, making it ideal for assessing reasoning capabilities of MLLMs. For ReVOS, we uniformly sample six frames and task the model with grounding one frame, deriving ground-truth bounding boxes from segmentation masks originally annotated for reasoning tasks.

To demonstrate the generalizability of our RL training strategies across multi-image understanding tasks, we evaluate our approach on two additional benchmarks: BLINK [9] and MMIU [26]. For BLINK, we assess performance on seven relevant subsets. For MMIU, we evaluate on four relevant types: low-level semantic relations, high-level semantic relationships (objective), high-level semantic relationships (subjective), and two-dimensional spatial relationships.

Training Configurations In the cold start CoT-SFT stage, we employ a learning rate of 1e-4 with cosine decay scheduling and an accumulated total batch size of 32. The maximum sequence length for generation is set to 1,024 tokens. During this phase, we freeze the vision encoder and MLP projector, updating only the LLM parameters via LoRA. For the subsequent RL phase, we only train the LLM. We set a learning rate of 5e-5 with 8 rollout samples per input, a batch size of 2, and gradient accumulation steps of 4. The reward weights λ_{acc} and λ_{format} are set to 1.0 and 0.5, respectively. The KL penalty coefficient β is set to 0.001, the sampling temperature to 0.7, and the output length remains 1024 tokens. All experiments are conducted with H800-80G GPUs.

Baselines We select several open-source MLLMs for comparison, such as Qwen2-VL [37], Qwen2.5-VL [1], InternVL2 [3], InternVL3 [51], LLaVA-OneVision [16], MiniCPM2.6 [43], and mPLUG-Owl3 [44]. To further verify the effectiveness of the RL paradigm, we compare our method with the SFT baseline, which is trained on the same dataset as our stage-1 CoT-SFT with a learning rate of 2e-6 and an accumulated batch size of 64.

Evaluation Metrics We employ the standard Acc@0.5 metric for the grounding task, which considers a prediction correct if its Intersection over Union (IoU) with the ground truth exceeds 0.5.

4.2 Comparison Results

MIG-Bench Comparison As shown in Table 2, we present the comparison results in the multi-image grounding benchmark MIG-Bench [19]. Our method achieves state-of-the-art performance

Model	Counting	Forensic	IQ	Jigsaw	Multi-view	Similarity	Vis.	Corr.	AVG
<i>Closed-source Model</i>									
GPT4o	49.17	79.55	<u>31.33</u>	55.33	<u>59.40</u>	72.59	75.00	<u>60.34</u>	
<i>Open-source Model</i>									
Qwen2.5-VL-7B + SFT-63k	<u>67.50</u> 63.33	45.45 32.58	27.33 26.67	<u>63.33</u> 72.67	<u>51.88</u> 48.12	82.96 90.37	68.02 62.21	58.07 56.56	
Ours-new	70.00	<u>47.73</u>	32.00	74.67	49.62	84.44	<u>69.77</u>	61.18	

Table 6: **Performance on Multi-image Understanding Benchmark BLINK [9].** Forensic, IQ, Multi-view, Similarity, and Vis. Corr. denote Forensic detection, IQ test, Multi-view reasoning, Visual similarity, and Vision Correspondence, respectively. The best and second-best results are marked in **bold** and underline, respectively. Results for GPT4o [27] are borrowed from BLINK.

Model	High-level Obj.					High-level Sub.			Low-level		AVG
	VGR	STS	VCor	SC	FC	ER	CR	MIC	VQA	FD	
<i>Closed-source Model</i>											
GPT4o	61.3	84.0	72.6	41.5	42.6	46.5	67.8	93.5	79.2	88.8	67.8
<i>Open-source Model</i>											
Mantis	65.2	65.5	30.9	28.1	24.3	31.8	61.5	71.0	59.8	57.0	49.5
Llava-interleave	49.8	54.5	25.1	26.4	23.2	24.8	29.5	57.0	48.8	26.3	36.5
Qwen2.5-VL-7B + SFT	68.0 <u>67.0</u>	74.0 80.0	44.6 40.3	33.6 28.6	25.1 <u>26.1</u>	31.0 <u>32.5</u>	57.0 <u>69.2</u>	80.0 87.5	82.8 81.2	72.0 65.1	56.8 <u>57.7</u>
Ours	66.8	72.0	51.1	<u>30.4</u>	27.0	39.0	69.5	87.0	<u>82.2</u>	<u>69.3</u>	59.4

Table 7: **Performance on Multi-image Understanding Benchmark MMIU [26].** High-level Obj. and High-level Sub. are represented as subtypes of high-level semantic relationship (objective) and high-level semantic relationship (subjective). The term "Low-level" denotes the subtype of low-level semantic relations. Some results are borrowed from the original paper. The best and second-best results among open-source models are marked in **bold** and underline, respectively.

overall. Specifically, it obtains the best results across all seven subsets of referential grounding. Compared to the base model (Qwen2.5-VL-7B), our approach achieves a 45.64% improvement, and it outperforms the second-best model (Qwen2.5-VL-72B) by 12.60%, while using significantly fewer parameters.

Moreover, we conduct a comprehensive comparison of various post-training strategies on both in-domain and out-of-domain tasks, shown in Table 3. The results reveal that conventional SFT training significantly improves in-domain performance but provides limited benefits for out-of-domain generalization. CoT-SFT training strategy enhances out-of-domain generalization to a certain extent but slightly compromises in-domain accuracy. Conversely, the RL training strategy achieves superior performance, obtaining the highest scores in both in-domain and out-of-domain settings, with a notable 53.34% on out-of-domain tasks. The results demonstrate the strong generalization capability of our approach across both conventional and novel task domains.

Zero-shot Evaluation To further highlight the robust generalization capability of our method, we conduct zero-shot evaluation on multiple datasets spanning different tasks: the single-image grounding dataset Ref-L4 [2], LISA [15], and the video grounding dataset ReVOS [40]. As illustrated in Table 4, our method consistently outperforms all baselines across multiple benchmarks. Although the SFT training strategy achieves slight overall improvements, it exhibits a severe performance drop on the LISA benchmark. It suggests that the SFT training method lacks strong generalization, relying on memorizing answers instead of learning underlying patterns. On the other hand, our RL training strategy, which is initialized with a small amount of data, achieves a substantial improvement of 4.98% over the SFT baseline and even surpasses the performance of Qwen2.5-VL-72B by 3.56%.

Model	Two-dimensional spatial relationship									AVG
	RPM	JPS	ICSC	IQASC	ITRSC	ISTE	HE	PT	SOT	
<i>Closed-source Model</i>										
GPT4o	12.5	23.5	58.5	88.0	17.5	35.0	29.5	55.0	56.0	41.7
<i>Open-source Model</i>										
Mantis	13.5	<u>27.5</u>	48.0	66.0	13.0	23.5	23.0	<u>76.0</u>	50.0	37.8
Llava-interleave	<u>15.0</u>	17.5	47.5	42.0	14.0	22.5	21.5	79.0	60.5	35.5
Qwen2.5-VL-7B	13.0	26.5	<u>55.5</u>	<u>75.5</u>	7.0	29.0	<u>23.5</u>	58.5	<u>55.5</u>	37.8
+ SFT	12.5	30.5	54.0	73.0	19.5	33.5	29.5	43.0	52.5	<u>38.6</u>
Ours	15.0	24.5	68.0	83.5	<u>19.0</u>	32.5	22.0	50.0	49.5	40.4

Table 8: **Performance on Multi-image Understanding Benchmark MMIU [26]** for two-dimensional spatial relationship subtype. Some results are borrowed from the original paper. The best and second-best results among open-source models are marked in **bold** and underline, respectively.

Ablation	Setting			Spontaneous Grounding			Referential Grounding						AVG	
	CS	RS	RL	Static	Robust	Common	OT	MV	Region	Refer	GG	Reason	Co-Re	
Qwen2.5-VL-7B	-	-	-	28.03	5.32	21.81	15.23	5.56	0.54	13.13	32.26	3.96	2.56	14.05
w/o CS	<u>✗</u>	<u>✗</u>	<u>✓</u>	31.25	7.45	38.73	14.77	5.56	11.59	18.18	36.07	10.89	3.42	17.79
CoT-SFT	<u>✓</u>	<u>✗</u>	<u>✗</u>	<u>47.35</u>	45.74	76.59	46.14	34.03	28.93	<u>80.81</u>	63.93	<u>66.34</u>	<u>34.19</u>	52.41
w/o RS	<u>✓</u>	<u>✗</u>	<u>✓</u>	47.16	46.81	80.39	50.23	<u>34.38</u>	<u>43.75</u>	79.80	<u>67.94</u>	67.33	<u>34.19</u>	55.20
Ours-Full	<u>✓</u>	<u>✓</u>	<u>✓</u>	51.52	<u>43.62</u>	82.48	63.41	38.54	47.89	82.83	69.54	67.33	<u>37.61</u>	58.47

Table 9: **Ablations on MIG-Bench.** CS and RS are represented as cold-start and rejection sampling. RL denotes Reinforcement learning.

Out-of-domain Object Detection The evaluation results on out-of-domain object detection task are presented in Table 5. As described in Section 4.1, we evaluate on five non-overlapping datasets from ODNIW, comprising 6,314 samples. Our full model achieves the highest average performance (54.15%) across all five datasets, surpassing the base model Qwen2.5-VL-7B by a significant improvement of 7.24%. Notably, it also outperforms both the SFT baseline and the largest scale base model, Qwen2.5-VL-72B. It demonstrate the robustness and strong generalization capability of our approach in handling out-of-domain object detection tasks.

Multi-image Understanding Evaluation Our method not only advances multi-image reasoning and grounding capabilities but also exhibits exceptional generalization in the multi-image understanding task. For comprehensive evaluation, we conduct extensive experiments on the BLINK [9] benchmark, with seven representative subsets: Counting, Forensic Detection, IQ Test, Jigsaw, Multi-view Reasoning, Visual Similarity, and Visual Correspondence. As shown in Table 6, our RL-based method achieves state-of-the-art performance, outperforming both the base model Qwen2.5-VL-7B [1] and the SFT baseline. What’s more, our method surpasses even the closed-source GPT-4o model [27], establishing new performance standards in multi-image understanding. Notably, although our post-training dataset includes only grounding tasks, the model demonstrates remarkable performance on multi-image understanding tasks. It reveals that the reasoning process during reinforcement learning can enhance the multi-image comprehension capabilities of the model.

For comprehensive evaluation on the MMIU [26] benchmark, we assess performance across semantic relationships and two-dimensional spatial relationships, as shown in Table 7 and Table 8, respectively. We compare our method with several closed-source models: GPT4o [27], open-source models: Mantis [13], Llava-interleave [17], and base model Qwen2.5-VL-7B [1]. We achieve the best performance among open-source models across all types.

4.3 Ablation Studies

To demonstrate the effectiveness of our approach, we perform ablation studies on MIG-Bench [19], shown in Table 9.

Effectiveness of Cold Start on GPRO As discussed in Section 3.2, we directly apply GRPO-based reinforcement learning following the DeepSeek-R1-Zero framework [10]. However, this attempt yields only minor performance gains, primarily due to the base model’s constraints in multi-image contexts and complex queries. These limitations underscore the critical importance of implementing a CoT-based cold-start strategy to establish a strong initialization for subsequent reward-based RL learning.

Effectiveness of Rejection Sampling Another key component of our approach is the data filtering via rejection sampling. To assess its impact, we conduct an ablation study by training the stage-1 CoT-SFT model directly with the GRPO algorithm, removing the rejection sampling process. As illustrated in the fourth row of Table 9, our full model—with rejection sampling enabled—achieves a improvement of 3.27%. It shows the importance of data quality in reinforcement learning training and demonstrates the effectiveness of our rejection sampling procedure.

5 Conclusion

In this paper, we aim to enhance the reasoning and understanding capabilities of MLLMs for real-world multi-image grounding applications. To this end, we propose a post-training strategy incorporating cold-start initialization to establish correct reasoning pathways, complemented by rule-based reinforcement learning to further strengthen the model’s reasoning abilities. Experimental results demonstrate that our approach significantly outperforms both the base model and the baseline SFT method across multiple multi-image grounding and understanding benchmarks. We hope this work will stimulate further research in the multi-image reasoning and grounding community.

References

- [1] Shuai Bai, Keqin Chen, Xuejing Liu, Jialin Wang, Wenbin Ge, Sibo Song, Kai Dang, Peng Wang, Shijie Wang, Jun Tang, et al. Qwen2. 5-vl technical report. *arXiv preprint arXiv:2502.13923*, 2025.
- [2] Jierun Chen, Fangyun Wei, Jinjing Zhao, Sizhe Song, Bohuai Wu, Zhuoxuan Peng, S-H Gary Chan, and Hongyang Zhang. Revisiting referring expression comprehension evaluation in the era of large multimodal models. In *Proceedings of the Computer Vision and Pattern Recognition Conference*, pages 513–524, 2025.
- [3] Zhe Chen, Jiannan Wu, Wenhui Wang, Weijie Su, Guo Chen, Sen Xing, Muyan Zhong, Qinglong Zhang, Xizhou Zhu, Lewei Lu, et al. Internvl: Scaling up vision foundation models and aligning for generic visual-linguistic tasks. In *Proceedings of the IEEE/CVF conference on computer vision and pattern recognition*, pages 24185–24198, 2024.
- [4] Tianzhe Chu, Yuexiang Zhai, Jihan Yang, Shengbang Tong, Saining Xie, Dale Schuurmans, Quoc V Le, Sergey Levine, and Yi Ma. Sft memorizes, rl generalizes: A comparative study of foundation model post-training. *arXiv preprint arXiv:2501.17161*, 2025.
- [5] Huilin Deng, Ding Zou, Rui Ma, Hongchen Luo, Yang Cao, and Yu Kang. Boosting the generalization and reasoning of vision language models with curriculum reinforcement learning. *arXiv preprint arXiv:2503.07065*, 2025.
- [6] Yihe Deng, Hritik Bansal, Fan Yin, Nanyun Peng, Wei Wang, and Kai-Wei Chang. Open-vlthinker: An early exploration to complex vision-language reasoning via iterative self-improvement. *arXiv preprint arXiv:2503.17352*, 2025.
- [7] Ahmed El-Kishky, Alexander Wei, Andre Saraiva, Borys Minaiev, Daniel Selsam, David Dohan, Francis Song, Hunter Lightman, Ignasi Clavera, Jakub Pachocki, et al. Competitive programming with large reasoning models. *arXiv preprint arXiv:2502.06807*, 2025.
- [8] Kaituo Feng, Kaixiong Gong, Bohao Li, Zonghao Guo, Yibing Wang, Tianshuo Peng, Junfei Wu, Xiaoying Zhang, Benyou Wang, and Xiangyu Yue. Video-r1: Reinforcing video reasoning in mllms. *arXiv preprint arXiv:2503.21776*, 2025.

[9] Xingyu Fu, Yushi Hu, Bangzheng Li, Yu Feng, Haoyu Wang, Xudong Lin, Dan Roth, Noah A Smith, Wei-Chiu Ma, and Ranjay Krishna. Blink: Multimodal large language models can see but not perceive. In *European Conference on Computer Vision*, pages 148–166. Springer, 2024.

[10] Daya Guo, Dejian Yang, Haowei Zhang, Junxiao Song, Ruoyu Zhang, Runxin Xu, Qihao Zhu, Shirong Ma, Peiyi Wang, Xiao Bi, et al. Deepseek-r1: Incentivizing reasoning capability in llms via reinforcement learning. *arXiv preprint arXiv:2501.12948*, 2025.

[11] Wenzuan Huang, Bohan Jia, Zijie Zhai, Shaosheng Cao, Zheyu Ye, Fei Zhao, Zhe Xu, Yao Hu, and Shaohui Lin. Vision-r1: Incentivizing reasoning capability in multimodal large language models. *arXiv preprint arXiv:2503.06749*, 2025.

[12] Aaron Jaech, Adam Kalai, Adam Lerer, Adam Richardson, Ahmed El-Kishky, Aiden Low, Alec Helyar, Aleksander Madry, Alex Beutel, Alex Carney, et al. Openai o1 system card. *arXiv preprint arXiv:2412.16720*, 2024.

[13] Dongfu Jiang, Xuan He, Huaye Zeng, Cong Wei, Max Ku, Qian Liu, and Wenhui Chen. Mantis: Interleaved multi-image instruction tuning. *arXiv preprint arXiv:2405.01483*, 2024.

[14] Yang Jiao, Shaoxiang Chen, Zequn Jie, Jingjing Chen, Lin Ma, and Yu-Gang Jiang. Lumen: Unleashing versatile vision-centric capabilities of large multimodal models. *arXiv preprint arXiv:2403.07304*, 2024.

[15] Xin Lai, Zhuotao Tian, Yukang Chen, Yanwei Li, Yuhui Yuan, Shu Liu, and Jiaya Jia. Lisa: Reasoning segmentation via large language model. In *Proceedings of the IEEE/CVF Conference on Computer Vision and Pattern Recognition*, pages 9579–9589, 2024.

[16] Bo Li, Yuanhan Zhang, Dong Guo, Renrui Zhang, Feng Li, Hao Zhang, Kaichen Zhang, Peiyuan Zhang, Yanwei Li, Ziwei Liu, et al. Llava-onevision: Easy visual task transfer. *arXiv preprint arXiv:2408.03326*, 2024.

[17] Feng Li, Renrui Zhang, Hao Zhang, Yuanhan Zhang, Bo Li, Wei Li, Zejun Ma, and Chunyuan Li. Llava-next-interleave: Tackling multi-image, video, and 3d in large multimodal models. *arXiv preprint arXiv:2407.07895*, 2024.

[18] Liunian Harold Li, Pengchuan Zhang, Haotian Zhang, Jianwei Yang, Chunyuan Li, Yiwu Zhong, Lijuan Wang, Lu Yuan, Lei Zhang, Jenq-Neng Hwang, et al. Grounded language-image pre-training. In *Proceedings of the IEEE/CVF conference on computer vision and pattern recognition*, pages 10965–10975, 2022.

[19] You Li, Heyu Huang, Chi Chen, Kaiyu Huang, Chao Huang, Zonghao Guo, Zhiyuan Liu, Jinan Xu, Yuhua Li, Ruixuan Li, et al. Magician: Revealing the magic of free-form multi-image grounding in multimodal large language models. *arXiv preprint arXiv:2501.05767*, 2025.

[20] Zhaowei Li, Qi Xu, Dong Zhang, Hang Song, Yiqing Cai, Qi Qi, Ran Zhou, Junting Pan, Zefeng Li, Van Tu Vu, et al. Groundinggpt: Language enhanced multi-modal grounding model. *arXiv preprint arXiv:2401.06071*, 2024.

[21] Zhenyi Liao, Qingsong Xie, Yanhao Zhang, Zijian Kong, Haonan Lu, Zhenyu Yang, and Zhijie Deng. Improved visual-spatial reasoning via r1-zero-like training. *arXiv preprint arXiv:2504.00883*, 2025.

[22] Haotian Liu, Chunyuan Li, Qingyang Wu, and Yong Jae Lee. Visual instruction tuning. *Advances in neural information processing systems*, 36:34892–34916, 2023.

[23] Yuqi Liu, Bohao Peng, Zhisheng Zhong, Zihao Yue, Fanbin Lu, Bei Yu, and Jiaya Jia. Seg-zero: Reasoning-chain guided segmentation via cognitive reinforcement. *arXiv preprint arXiv:2503.06520*, 2025.

[24] Ziyu Liu, Zeyi Sun, Yuhang Zang, Xiaoyi Dong, Yuhang Cao, Haodong Duan, Dahua Lin, and Jiaqi Wang. Visual-rft: Visual reinforcement fine-tuning. *arXiv preprint arXiv:2503.01785*, 2025.

[25] Junhua Mao, Jonathan Huang, Alexander Toshev, Oana Camburu, Alan L Yuille, and Kevin Murphy. Generation and comprehension of unambiguous object descriptions. In *Proceedings of the IEEE conference on computer vision and pattern recognition*, pages 11–20, 2016.

[26] Fanqing Meng, Jin Wang, Chuanhao Li, Quanfeng Lu, Hao Tian, Jiaqi Liao, Xizhou Zhu, Jifeng Dai, Yu Qiao, Ping Luo, et al. Mmiu: Multimodal multi-image understanding for evaluating large vision-language models. *arXiv preprint arXiv:2408.02718*, 2024.

[27] OpenAI. Gpt-4o. <https://openai.com/index/hello-gpt-4o/>, 2024.

[28] Long Ouyang, Jeffrey Wu, Xu Jiang, Diogo Almeida, Carroll Wainwright, Pamela Mishkin, Chong Zhang, Sandhini Agarwal, Katarina Slama, Alex Ray, et al. Training language models to follow instructions with human feedback. *Advances in neural information processing systems*, 35:27730–27744, 2022.

[29] Yi Peng, Xiaokun Wang, Yichen Wei, Jiangbo Pei, Weijie Qiu, Ai Jian, Yunzhuo Hao, Jiachun Pan, Tianyidan Xie, Li Ge, et al. Skywork r1v: Pioneering multimodal reasoning with chain-of-thought. *arXiv preprint arXiv:2504.05599*, 2025.

[30] Rafael Rafailov, Archit Sharma, Eric Mitchell, Christopher D Manning, Stefano Ermon, and Chelsea Finn. Direct preference optimization: Your language model is secretly a reward model. *Advances in Neural Information Processing Systems*, 36:53728–53741, 2023.

[31] Hanoona Rasheed, Muhammad Maaz, Sahal Shaji, Abdelrahman Shaker, Salman Khan, Hisham Cholakkal, Rao M Anwer, Eric Xing, Ming-Hsuan Yang, and Fahad S Khan. Glamm: Pixel grounding large multimodal model. In *Proceedings of the IEEE/CVF Conference on Computer Vision and Pattern Recognition*, pages 13009–13018, 2024.

[32] Zhihong Shao, Peiyi Wang, Qihao Zhu, Runxin Xu, Junxiao Song, Xiao Bi, Haowei Zhang, Mingchuan Zhang, YK Li, Y Wu, et al. Deepseekmath: Pushing the limits of mathematical reasoning in open language models. *arXiv preprint arXiv:2402.03300*, 2024.

[33] Haozhan Shen, Peng Liu, Jingcheng Li, Chunxin Fang, Yibo Ma, Jiajia Liao, Qiaoli Shen, Zilun Zhang, Kangjia Zhao, Qianqian Zhang, et al. Vlm-r1: A stable and generalizable r1-style large vision-language model. *arXiv preprint arXiv:2504.07615*, 2025.

[34] Huajie Tan, Yuheng Ji, Xiaoshuai Hao, Minglan Lin, Pengwei Wang, Zhongyuan Wang, and Shanghang Zhang. Reason-rft: Reinforcement fine-tuning for visual reasoning. *arXiv preprint arXiv:2503.20752*, 2025.

[35] Kimi Team, Angang Du, Bofei Gao, Bowei Xing, Changjiu Jiang, Cheng Chen, Cheng Li, Chenjun Xiao, Chenzhuang Du, Chonghua Liao, et al. Kimi k1. 5: Scaling reinforcement learning with llms. *arXiv preprint arXiv:2501.12599*, 2025.

[36] Jiaqi Wang, Pan Zhang, Tao Chu, Yuhang Cao, Yujie Zhou, Tong Wu, Bin Wang, Conghui He, and Dahua Lin. V3det: Vast vocabulary visual detection dataset. In *Proceedings of the IEEE/CVF International Conference on Computer Vision*, pages 19844–19854, 2023.

[37] Peng Wang, Shuai Bai, Sinan Tan, Shijie Wang, Zhihao Fan, Jinze Bai, Kejin Chen, Xuejing Liu, Jialin Wang, Wenbin Ge, et al. Qwen2-vl: Enhancing vision-language model’s perception of the world at any resolution. *arXiv preprint arXiv:2409.12191*, 2024.

[38] Ye Wang, Ziheng Wang, Boshen Xu, Yang Du, Kejun Lin, Zihan Xiao, Zihao Yue, Jianzhong Ju, Liang Zhang, Dingyi Yang, et al. Time-r1: Post-training large vision language model for temporal video grounding. *arXiv preprint arXiv:2503.13377*, 2025.

[39] Guowei Xu, Peng Jin, Li Hao, Yibing Song, Lichao Sun, and Li Yuan. Llava-o1: Let vision language models reason step-by-step. *arXiv preprint arXiv:2411.10440*, 2024.

[40] Cilin Yan, Haochen Wang, Shilin Yan, Xiaolong Jiang, Yao Hu, Guoliang Kang, Weidi Xie, and Efstratios Gavves. Visa: Reasoning video object segmentation via large language models. In *European Conference on Computer Vision*, pages 98–115. Springer, 2024.

[41] An Yang, Anfeng Li, Baosong Yang, Beichen Zhang, Binyuan Hui, Bo Zheng, Bowen Yu, Chang Gao, Chengen Huang, Chenxu Lv, et al. Qwen3 technical report. *arXiv preprint arXiv:2505.09388*, 2025.

[42] Yi Yang, Xiaoxuan He, Hongkun Pan, Xiyan Jiang, Yan Deng, Xingtao Yang, Haoyu Lu, Dacheng Yin, Fengyun Rao, Minfeng Zhu, et al. R1-onevision: Advancing generalized multimodal reasoning through cross-modal formalization. *arXiv preprint arXiv:2503.10615*, 2025.

[43] Yuan Yao, Tianyu Yu, Ao Zhang, Chongyi Wang, Junbo Cui, Hongji Zhu, Tianchi Cai, Haoyu Li, Weilin Zhao, Zhihui He, et al. Minicpm-v: A gpt-4v level mllm on your phone. *arXiv preprint arXiv:2408.01800*, 2024.

[44] Jiabo Ye, Haiyang Xu, Haowei Liu, Anwen Hu, Ming Yan, Qi Qian, Ji Zhang, Fei Huang, and Jingren Zhou. mplug-owl3: Towards long image-sequence understanding in multi-modal large language models. *arXiv preprint arXiv:2408.04840*, 2024.

[45] En Yu, Kangheng Lin, Liang Zhao, Jisheng Yin, Yana Wei, Yuang Peng, Haoran Wei, Jianjian Sun, Chunrui Han, Zheng Ge, et al. Perception-r1: Pioneering perception policy with reinforcement learning. *arXiv preprint arXiv:2504.07954*, 2025.

[46] Licheng Yu, Patrick Poirson, Shan Yang, Alexander C Berg, and Tamara L Berg. Modeling context in referring expressions. In *Computer Vision–ECCV 2016: 14th European Conference, Amsterdam, The Netherlands, October 11–14, 2016, Proceedings, Part II 14*, pages 69–85. Springer, 2016.

[47] Yufei Zhan, Yousong Zhu, Hongyin Zhao, Fan Yang, Ming Tang, and Jinqiao Wang. Griffon v2: Advancing multimodal perception with high-resolution scaling and visual-language co-referring. *arXiv preprint arXiv:2403.09333*, 2024.

[48] Yufei Zhan, Yousong Zhu, Shurong Zheng, Hongyin Zhao, Fan Yang, Ming Tang, and Jinqiao Wang. Vision-r1: Evolving human-free alignment in large vision-language models via vision-guided reinforcement learning. *arXiv preprint arXiv:2503.18013*, 2025.

[49] Jingyi Zhang, Jiaxing Huang, Huanjin Yao, Shunyu Liu, Xikun Zhang, Shijian Lu, and Dacheng Tao. R1-vl: Learning to reason with multimodal large language models via step-wise group relative policy optimization. *arXiv preprint arXiv:2503.12937*, 2025.

[50] Xingjian Zhang, Siwei Wen, Wenjun Wu, and Lei Huang. Tinyllava-video-r1: Towards smaller lmms for video reasoning. *arXiv preprint arXiv:2504.09641*, 2025.

[51] Jinguo Zhu, Weiyun Wang, Zhe Chen, Zhaoyang Liu, Shenglong Ye, Lixin Gu, Hao Tian, Yuchen Duan, Weijie Su, Jie Shao, et al. Internvl3: Exploring advanced training and test-time recipes for open-source multimodal models. *arXiv preprint arXiv:2504.10479*, 2025.